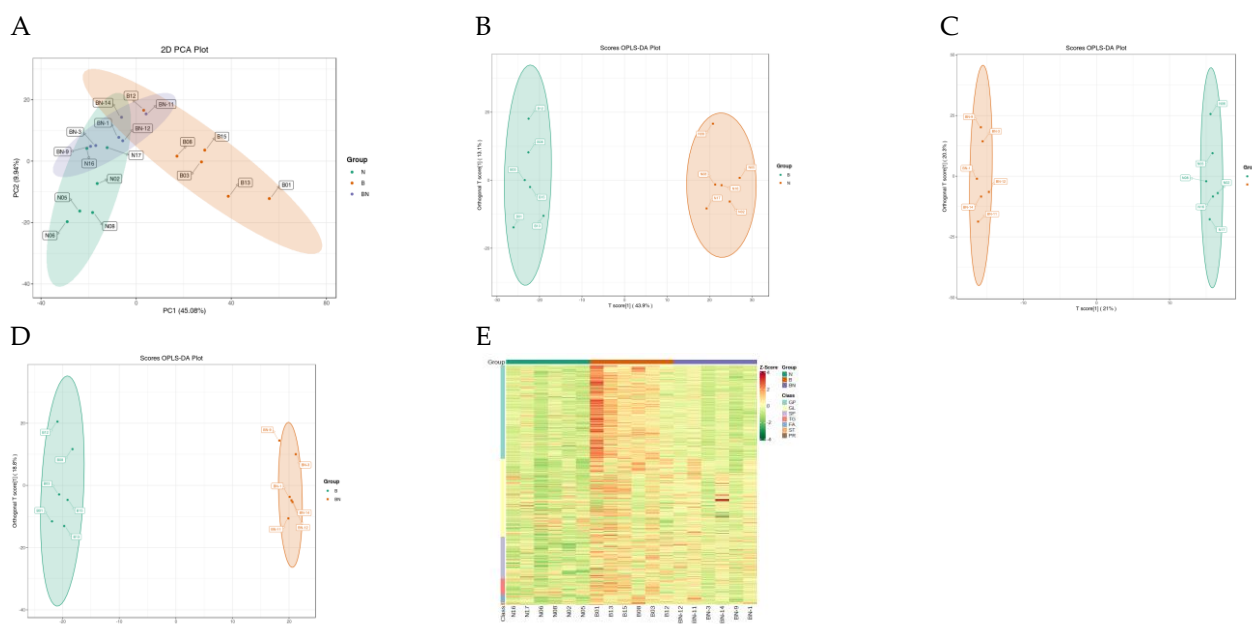
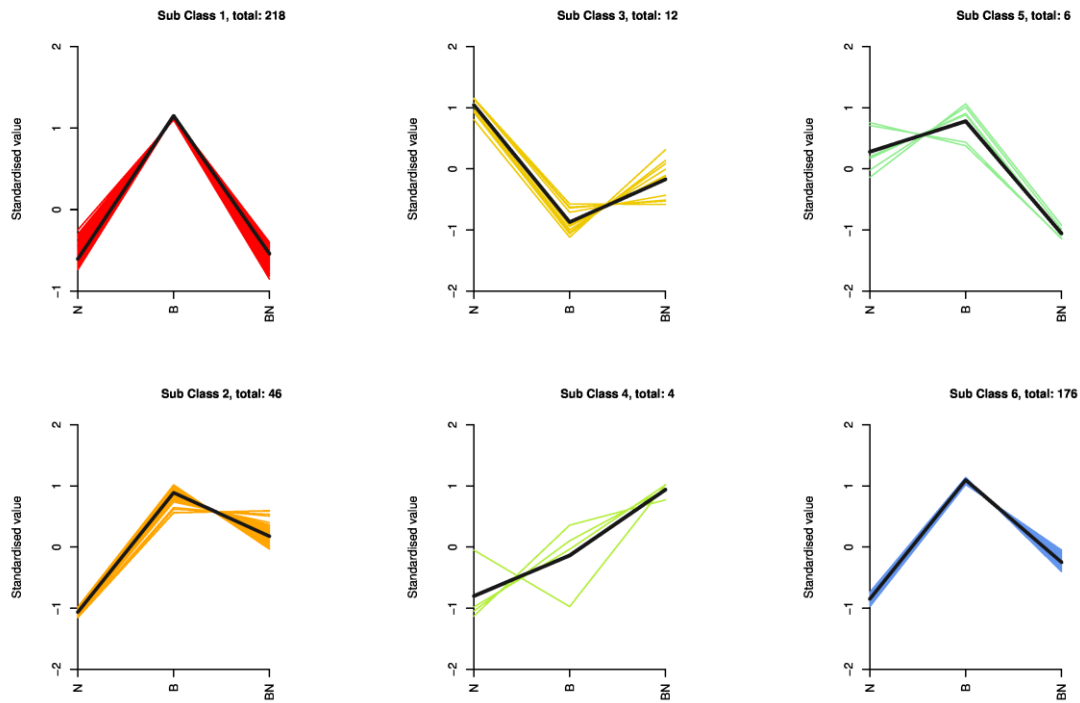


**Figure S1.** Ring diagram of lipid subclass composition, 18 samples of subcutaneous adipose from six Ningxiang pigs, six Berkshires and six F<sub>1</sub> pigs, respectively, were used to detect lipidomic profile.



**Figure S2.** The subcutaneous adipose tissue lipid composition. (A) PCA of the subcutaneous adipose tissue from Ningxiang pigs, Berkshires and F<sub>1</sub> offspring. (B) OPLS-DA of the subcutaneous adipose tissue from Ningxiang pigs and Berkshires. (C) OPLS-DA of the subcutaneous adipose tissue from Ningxiang pigs and F<sub>1</sub> offspring. (D) OPLS-DA of the subcutaneous adipose tissue from Berkshires and F<sub>1</sub> offspring. (E) Overall cluster heat map of the samples. Eighteen samples of subcutaneous adipose from six Ningxiang pigs, six Berkshires and six F<sub>1</sub> pigs, respectively, were used to detect lipidomic profile.



**Figure S3.** K-Means of SCLs. The horizontal ordinate represents sample groups, the Y-axis represents standardized relative lipid content, and Sub Class represents lipid class numbers with the same trend of change. Twelve samples of subcutaneous adipose from four Ningxiang pigs, four Berkshires and four F<sub>1</sub> pigs, respectively, were used to detect transcriptomic profile. B, Berkshires; N, Ningxiang pigs; BN, F<sub>1</sub> offspring.

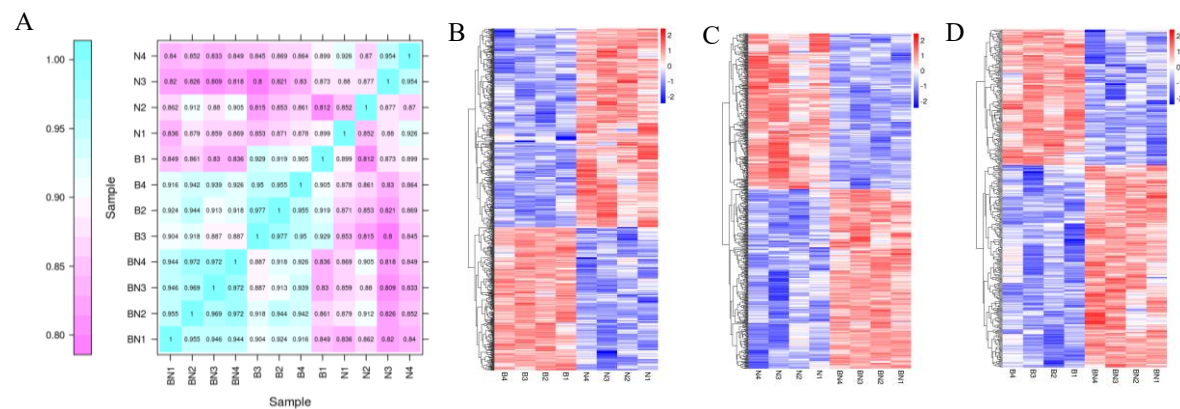
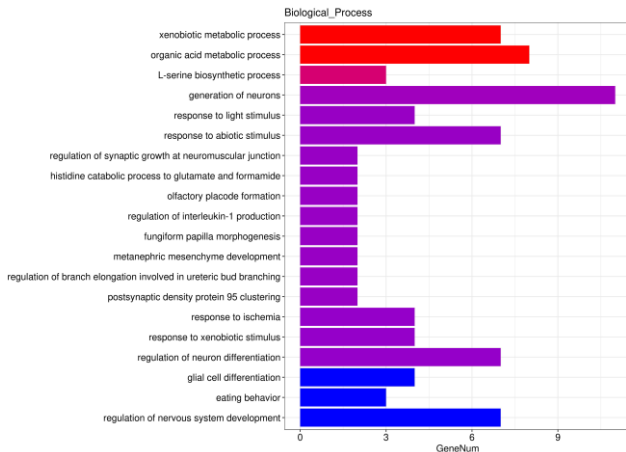
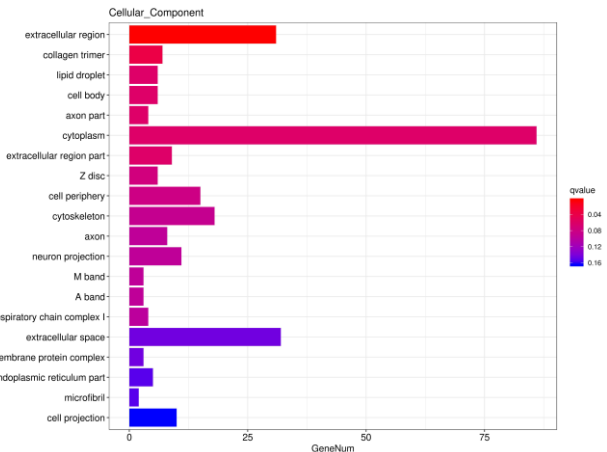


**Figure S4.** Transcriptome profiles diverse in the subcutaneous adipose tissue. (A) Transcriptome correlation analysis, B, Berkshire; N, Ningxiang pig; BN, F<sub>1</sub> offspring; (B-D) Cluster heat map of DEGs for the subcutaneous adipose tissue in the groups of Berkshires vs Ningxiang pigs (B), Ningxiang pigs vs F<sub>1</sub> offspring (C), Berkshires vs F<sub>1</sub> pigs (D). Twelve samples of subcutaneous adipose from four Ningxiang pigs, four Berkshires and four F<sub>1</sub> pigs, respectively, were used to detect transcriptomic profile. B, Berkshire; N, Ningxiang pig; BN, F<sub>1</sub> offspring.

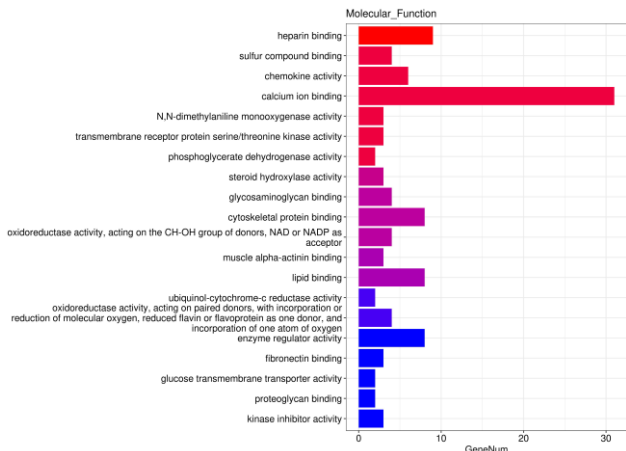
A



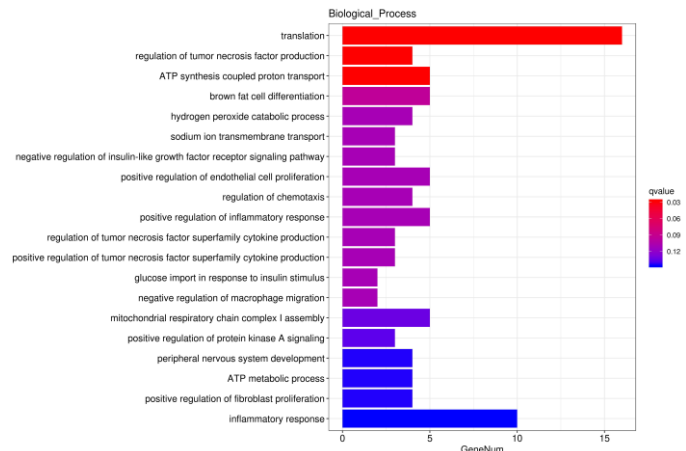
B



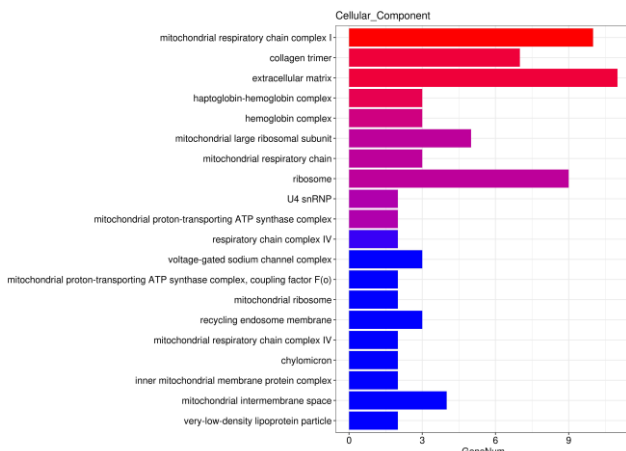
C



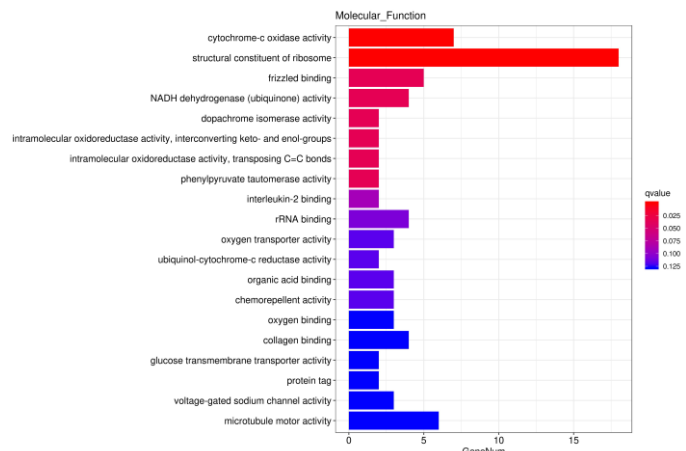
D



E

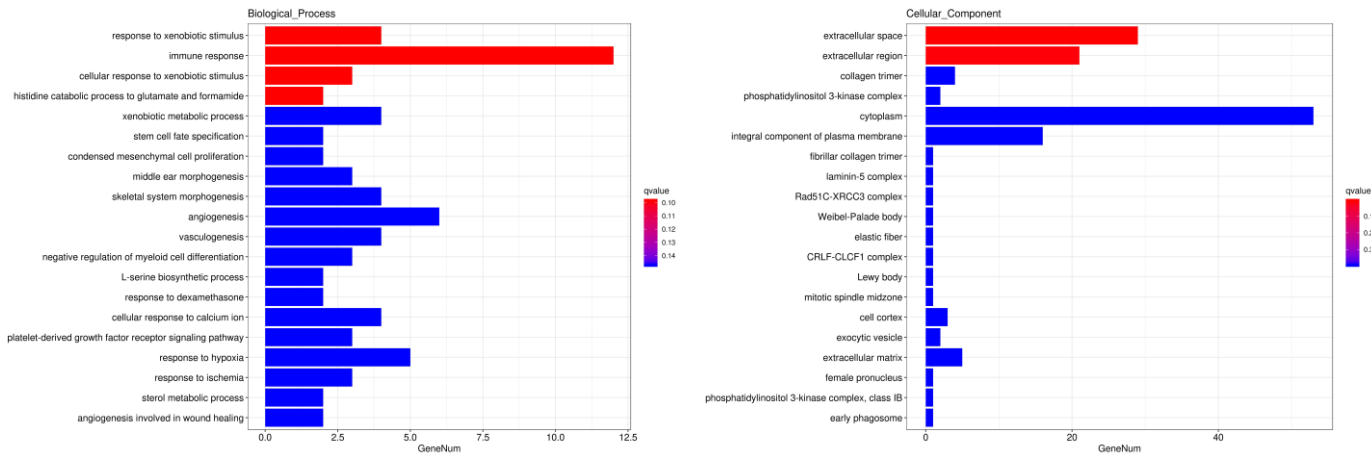


F



G

H



I

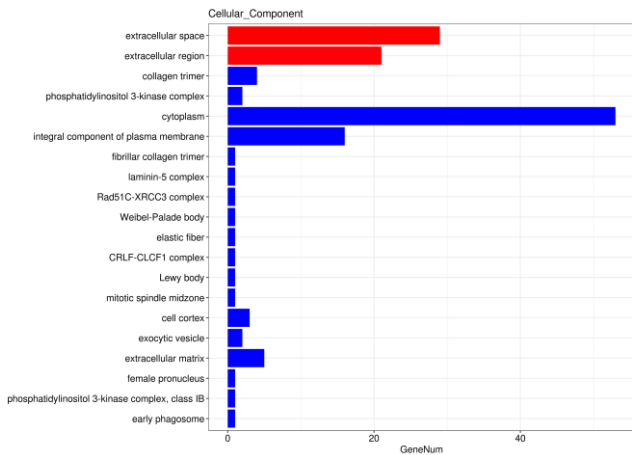
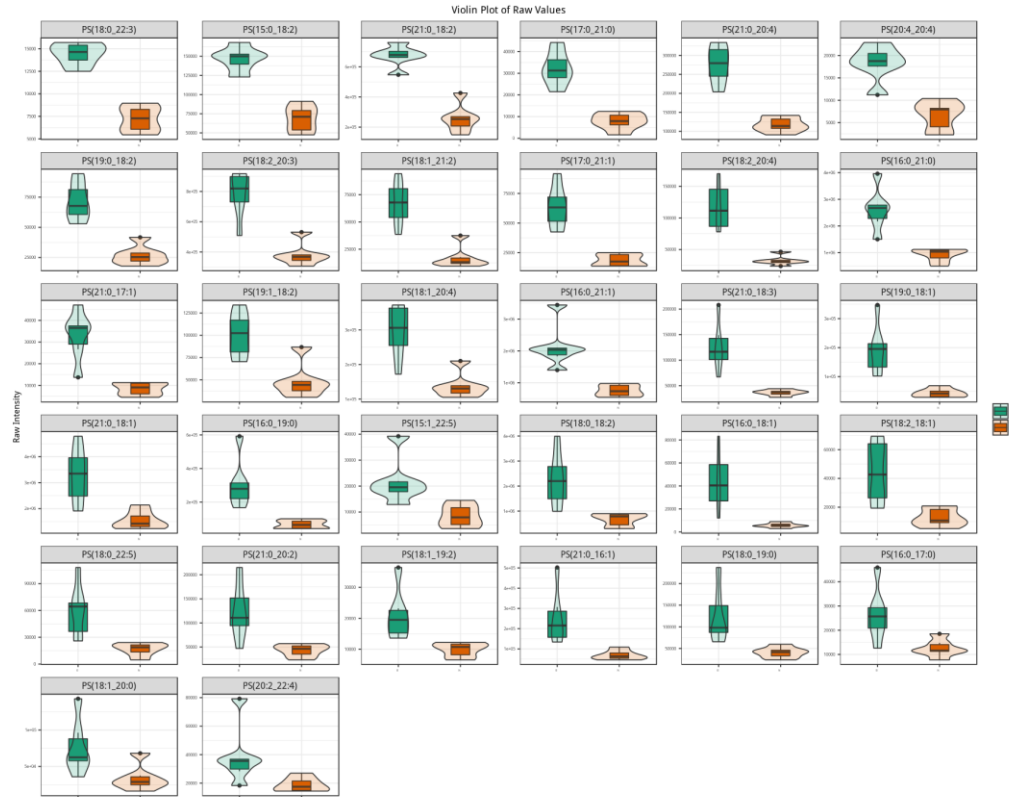


**Figure S5.** A partial list of bioinformatics analysis results using DEGs of the subcutaneous adipose tissue. (A-C) The column diagrams for the analysis of biological processes (A), cellular components (B), and molecular functions (C) of DEGs in Berkshires vs. Ningxiang pigs; (D-F) The column diagrams for the analysis of biological processes (D), cellular components (E), and molecular functions (F) of DEGs in Ningxiang pigs vs. F<sub>1</sub> offspring; (G-I) The column diagrams for the analysis of biological processes (G), cellular component (H), and molecular function (I) of DEGs in Berkshires vs. F<sub>1</sub> offspring. Twelve samples of subcutaneous adipose from four Ningxiang pigs, four Berkshires and four F<sub>1</sub> pigs, respectively, were used to detect transcriptomic profile.

A



B



**Figure S6.** The violin chart of the SCLs related to k00260 pathway. The violin chart of Phosphatidylserines in Berkshires vs. Ningxiang pigs (A) and Berkshires vs F1 offspring (B), respectively. B, Berkshires; N, Ningxiang pig; BN, F1 offspring.

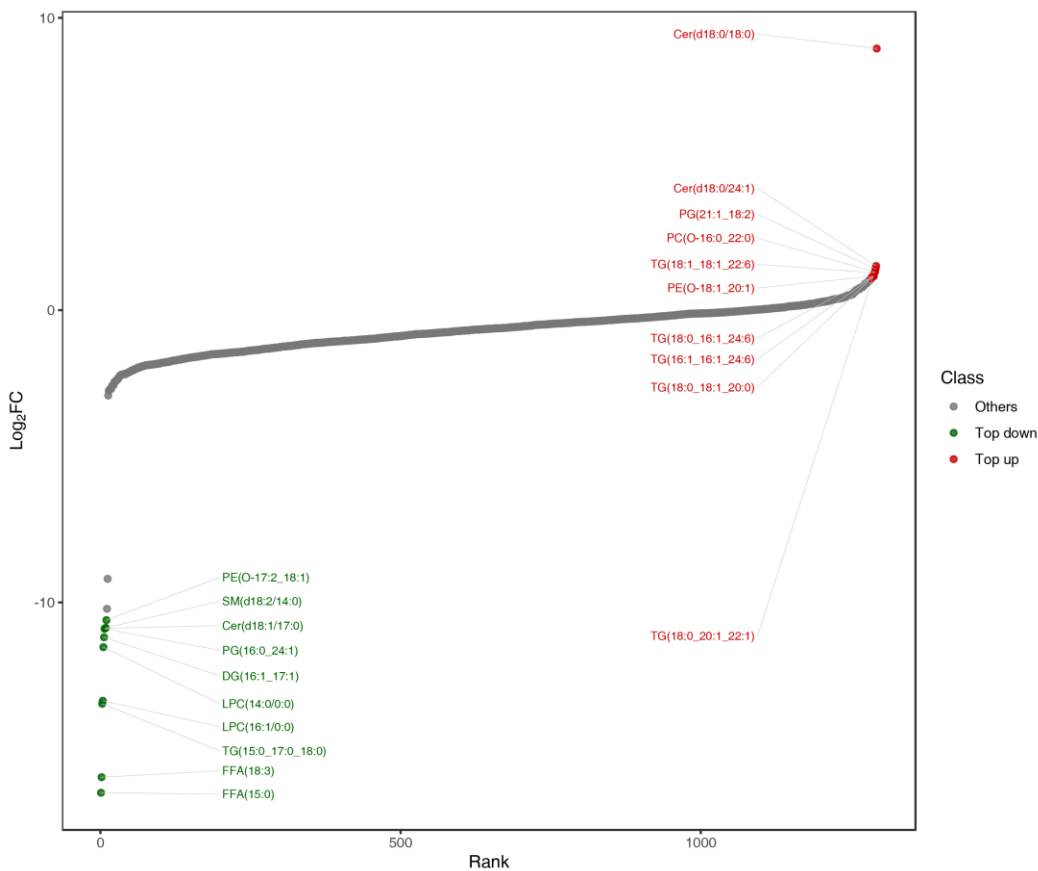


**Figure S7.** Dynamic distribution map of lipid content differences in the subcutaneous adipose tissue from Berkshires vs. Ningxiang pigs. The horizontal ordinate represents the different multiples of substances, the Y-axis represents the  $\log_2FC$ . Each point represents a substance, green dots represent the substances in the top 10 of the downward ranking, and red dots represent the substances in the top 10 of the upward ranking.

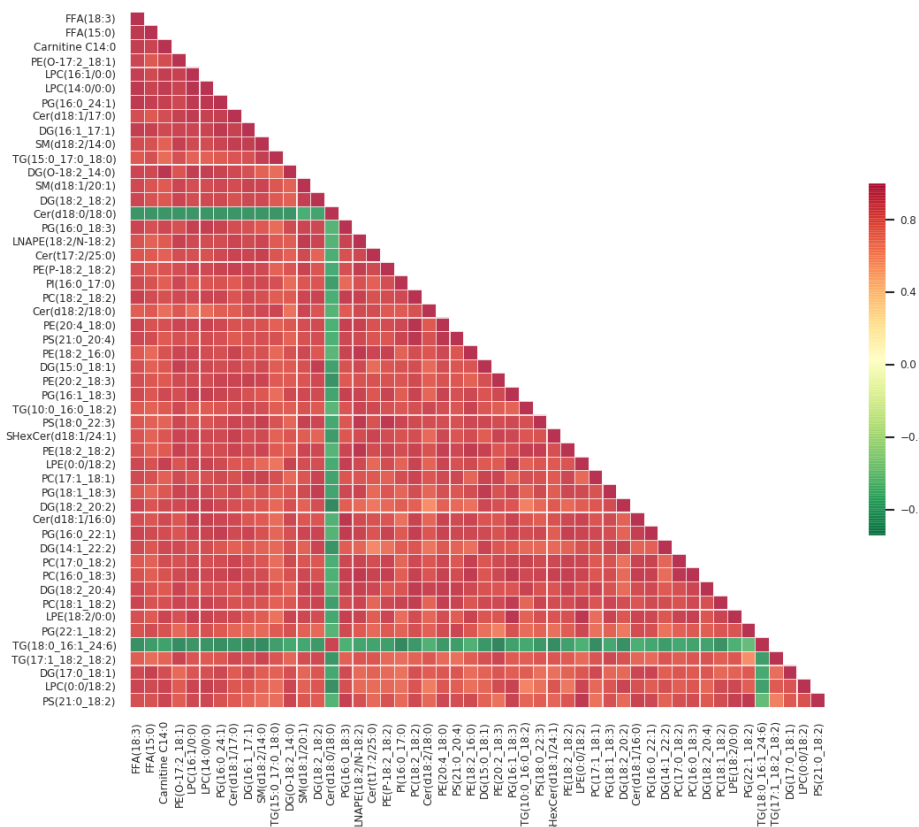


**Figure S8.** The correlation heat map for significantly different lipids with the top VIP value in the subcutaneous adipose tissue in Berkshires vs. Ningxiang pigs. Red represents positive correlations, green represents negative correlations.

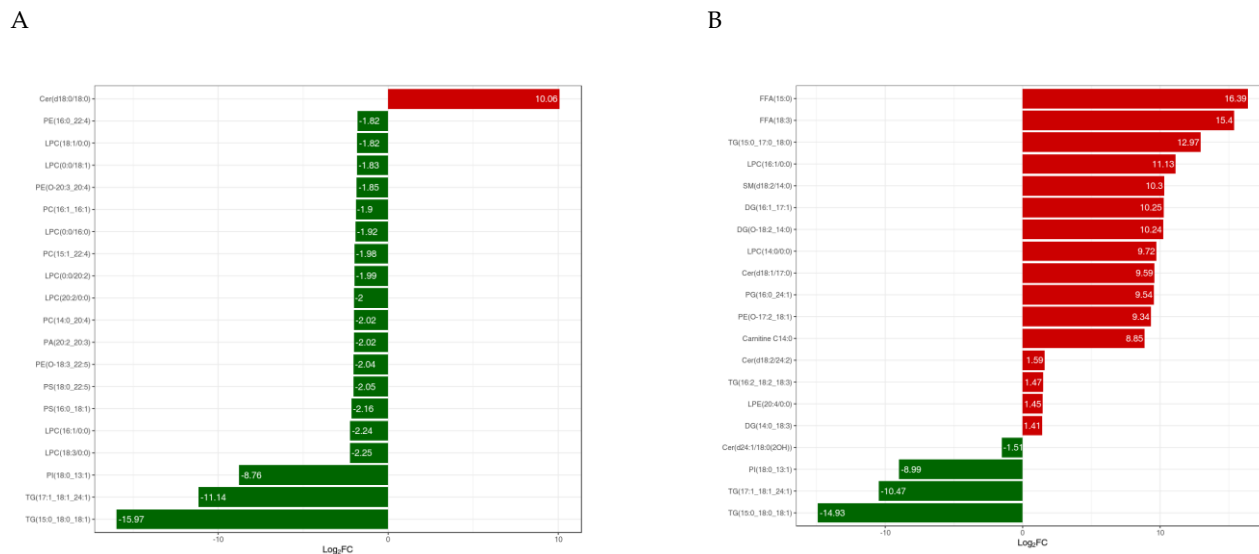


**Figure S9.** Bar chart of different lipids in the subcutaneous adipose tissue in Berkshires vs. F1 offspring (A) and in Ningxiang pigs vs. F1 offspring (B). The horizontal ordinate represents the log<sub>2</sub>FC of different lipids. The Y-axis represents differential lipids. Red represents an increase in lipid content, while green represents a decrease in lipid content.

**Table S1.** DEGs in Berkshires vs. Ningxiang pigs enriched in partial KEGG pathways ( $P < 0.05$ ).

Gene name	FPKM		FDR	Log2FC	regulate	Gene annotated
	BKX	NX				
<b>kO00260 glycine, serine and threonine metabolism</b>						
<i>PHGDH</i>	28.12	4.17	2.27E-11	-2.64	down	phosphoglycerate dehydrogenase
<i>LOC100156167</i>	8.84	1.44	3.84E-7	-2.41	down	phosphoglycerate dehydrogenase like protein
<i>SHMT1</i>	86.01	26.98	9.92E-4	-1.56	down	glycine hydroxymethyltransferase
<i>PSPH</i>	12.56	52.64	9.42E-6	2.21	up	phosphoserine phosphatase
<i>LOC110256000</i>	3.37	19.40	9.12E-08	2.49	up	membrane primary amine oxidase-like
<b>KO00590 arachidonic acid metabolism</b>						
<i>CYP2B22</i>	69.83	17.85	1.32E-3	-1.85	down	cytochrome P450 family 2 subfamily B22
<i>LOC110255237</i>	6.63	22.28	2.09E-4	1.86	up	cytochrome P450 4F6-like
<i>GGT5</i>	8.43	23.69	1.70E-3	1.54	up	gamma-glutamyltranspeptidase
<i>PTGES</i>	3.91	13.12	4.47E-8	1.86	up	microsomal prostaglandin-E synthase 1
<i>SAL1</i>	25.78	134.40	3.37E-6	2.45	up	salivary lipocalin
<i>GPX1</i>	334.05	1411.35	3.60E-7	2.20	up	glutathione peroxidase 1
<i>GPX3</i>	2304.61	1055.47	4.01E-7	-1.01	down	
<b>KO00061 fatty acid biosynthesis</b>						
<i>FASN</i>	1320.46	2689.93	1.19E-3	1.15	up	fatty acid synthase
<i>ACACA</i>	26.60	73.44	5.13E-9	1.58	up	acetyl-CoA carboxylase
<i>CBR4</i>	3.87	7.46	9.83E-6	1.06	up	carboxyl reductase 4
<i>MCH</i>	0.19	0.82	6.33E-3	2.20	up	medium chain acyl hydrolase
<b>KO01212 fatty acid metabolism</b>						
<i>EHHADH</i>	8.54	16.07	2.70E-3	1.03	up	enoyl-CoA hydratase
<i>FASN</i>	1320.46	2689.93	1.19E-3	1.15	up	fatty acid synthase

Gene name	FPKM		FDR	Log <sub>2</sub> FC	regulate	Gene annotated
	BKX	NX				
<i>ACACA</i>	26.60	73.44	5.13E <sup>-9</sup>	1.58	up	acetyl-CoA carboxylase
<i>CBR4</i>	3.87	7.46	9.83E <sup>-6</sup>	1.06	up	carboxyl reductase 4
<i>HACD</i>	98.60	42.53	7.91E <sup>-6</sup>	-1.10	down	very long-chain (3R)-3-hydroxyacyl-CoA dehydratase
<i>ELOV6</i>	182.38	428.54	9.82E <sup>-5</sup>	1.36	up	very long chain fatty acids protein 6
<i>SCD</i>	1184.93	3625.88	5.31E <sup>-5</sup>	1.75	up	stearoyl-CoA desaturase
<b>kO00561 glycerolipid metabolism</b>						
<i>GK</i>	23.72	8.19	5.06E <sup>-9</sup>	-1.37	down	glycerol kinase
<i>MGLL</i>	192.95	383.22	7.45E <sup>-10</sup>	1.04	up	monoglyceride lipase
<i>LPIN1</i>	127.44	44.92	5.42E <sup>-4</sup>	-1.40	down	lipin 1
<i>DGKB</i>	3.62	1.58	1.28E <sup>-3</sup>	-1.07	down	diacylglycerol kinase beta
<i>DGAT2</i>	109.71	518.44	8.38E <sup>-20</sup>	2.36	up	diacylglycerol O-acyltransferase 2
<b>ko04070 phosphatidylinositol signaling system</b>						
<i>NTMR7</i>	0.26	1.43	1.36E <sup>-3</sup>	2.54	up	myotubularin-related protein 7
<i>PLCB1</i>	4.49	2.06	1.14E <sup>-6</sup>	-1.01	down	phospholipase C beta 1
<i>PIK3C2G</i>	9.04	3.31	4.24E <sup>-14</sup>	-1.30	down	phosphatidylinositol-4-phosphate 3-kinase catalytic subunit type 2 gamma
<i>DGKB</i>	3.62	1.58	1.28E <sup>-3</sup>	-1.07	down	diacylglycerol kinase beta
<i>PLCE1</i>	0.45	0.19	4.25E <sup>-3</sup>	-1.11	down	phospholipase C epsilon 1
<i>CALML5</i>	2.09	0.13	6.52E <sup>-6</sup>	-3.91	down	calmodulin like 5
<i>LOC102157965</i>	0.15	1.53	2.35E <sup>-4</sup>	4.36	up	parvalbumin beta-like
<b>kO04973 carbohydrate digestion and absorption</b>						
<i>ATP1A1</i>	83.22	34.41	2.93E <sup>-7</sup>	-1.17	down	sodium/potassium-transporting ATPase subunit alpha1
<i>HK3</i>	4.41	9.39	6.21E <sup>-3</sup>	1.24	up	hexokinase3
<i>SLC2A5</i>	12.86	32.20	5.91E <sup>-3</sup>	1.44	up	Solute carrier family 2 member 5
<i>PLCB1</i>	4.49	2.06	1.14E <sup>-6</sup>	-1.01	down	phospholipase C beta 1
<b>kO04714 thermogenesis</b>						
<i>MGLL</i>	192.95	383.22	7.45E <sup>-10</sup>	1.04	up	acylglycerol lipase
<i>ATP5MC1</i>	79.10	148.15	7.42E <sup>-3</sup>	1.02	up	ATP synthase membrane subunit c locus 1
<i>UQCRC10</i>	63.91	150.00	2.65E <sup>-4</sup>	1.35	up	ubiquinol-cytochrome c complex III subunit X
<i>NDUFA3</i>	11.52	25.38	8.14E <sup>-3</sup>	1.26	up	NADH:ubiquinone oxidoreductase subunit A3
<i>UQCRCQ</i>	47.93	108.01	2.28E <sup>-6</sup>	1.29	up	ubiquinol-cytochrome c reductase complex III subunit VII
<i>COX7C</i>	134.91	329.31	2.04E <sup>-3</sup>	1.34	up	cytochrome c oxidase subunit 7C
<i>NDUFA11</i>	45.34	85.17	9.02E <sup>-5</sup>	1.03	up	NADH:ubiquinone oxidoreductase subunit A11
<i>NDUFB2</i>	39.84	81.82	2.27E <sup>-3</sup>	1.20	up	NADH:ubiquinone oxidoreductase subunit B2
<i>NDUFA2</i>	33.06	62.73	7.84E <sup>-8</sup>	1.04	up	NADH:ubiquinone oxidoreductase subunit A2
<i>COXI7</i>	41.24	105.00	4.63E <sup>-7</sup>	1.47	up	cytochrome c oxidase copper chaperone COX17
<i>UQCRC11</i>	1.27	7.07	2.71E <sup>-3</sup>	2.58	up	ubiquinol-cytochrome c reductase, complex III subunit XI

**Table S2.** Primers for real-time fluorescent quantitative PCR.

Gene	Primer sequence (5'-3')
<i>β-actin</i>	sense: CCAGGTCACTACCATCGG Antisense: CCGTGGCGTAGAGGT
<i>FASN</i>	sense: GGGCCCAGCATCACCATAGACA Antisense: GTTCGTGCCGCATTGAGGAT
<i>SCD</i>	sense: CTTCCTGATCATTGCCAACAA Antisense: GCAAACCACCCCTCTCTTG
<i>PSPH</i>	sense: GATGCTGTGTTGATGTTGAC Antisense: CTTGACTTGTGCCTGATCACATT
<i>ACACA</i>	sense: GTCCTCTGCCAGTTCCC Antisense: TCCATCACACAGCCTTC
<i>ELOV6</i>	sense: CCGGAAGTTGCCATGTTCA Antisense: GCAGAAGAGCACAAAGGTAGC
<i>HACD2</i>	sense: CAGACGGAGCTCTCTGG Antisense: TGTCTTCATTCTGGACCTCTCG
<i>GPX1</i>	sense: CAAGAATGGGGAGATCCTGA Antisense: GATAAACCTGGGTCGGTCA
<i>GPX3</i>	sense: CTCGGAGATTCTGTCCACTCTCA Antisense: CCGTTCACGTCCCCCTTCT
<i>LPIN1</i>	sense: GATCATCTCCGACATTGACG Antisense: TGGTACAGCTTGGCTATGC
<i>MGLL</i>	sense: TATGAGGGTGCGCTACAC Antisense: GTCCTTGAGGACCCAT
<i>CYP2B22</i>	sense: AGTGTGGAGAAGCACCGTGAA Antisense: GCAAAGAAGAGCGAAAGGACAGT
<i>DGAT2</i>	sense: TGGCTTTCCATTTCATCC Antisense: CGTAAGCACGATCAGAACGA